INFLUENCE OF GEOMETRY AND COOLING RATE ON PROPERTIES OF SINTER-HARDENED STEELS

Ilaria Forno [1)], Marco Actis Grande[1)]
[1)] Politecnico di Torino, Department of Applied Science and Technology, Alessandria, Italy

Received 14.03.2013
Accepted 18.07.2013

Corresponding author: *Ilaria Forno, E-mail address: ilaria.forno@polito.it, Tel.: +39-0131-229 252, Fax: +39-0131-229 399, Politecnico di Torino, Department of Applied Science and Technology, Viale T. Michel 5, 15121 Alessandria, Italy*

Abstract
The aim of this paper is to deepen the understanding of the influence of the cooling step on the final properties of sinter-hardened components, mainly focusing on part geometry (through the definition of an A/M ratio) and cooling rate. A commercial Distaloy DH powder has been uniaxially pressed in different shapes, identified in terms of area/mass index, at three different compacting pressures (500, 600 and 800 MPa). During the sinter-hardening process, conducted in a belt-furnace, temperature profiles and atmosphere have been sampled and analysed. Particular attention has been paid to the cooling step, carried out at different furnace settings (10 to 80% of the maximum cooling capability in terms of fan speed). Sintered samples have been analysed in terms of carbon and oxygen content, hardness and microstructure. The considered properties have then been compared with dilatometer data, derived from literature. Matching these properties, a correlation between furnace setting, shape and microstructure has been drawn.

Keywords: powder metallurgy, steel, sinter-hardening, geometry index

1 Introduction

Several approaches may be used to improve the properties/performances of Powder Metallurgy (PM) materials, both in terms of alloying elements added to the traditional powders available on the market [1-3], and by using properly designed (or adapted) sintering cycles [4, 5].
Sinter-hardening is a widely used, well-known process [6], aiming to enhance mechanical properties of sintered components, also when made up of modified alloy powder mixes [7], combining sintering and hardening in the same heat treatment.
In order to get high performance components it is possible to work on the hardening of the material, increasing the cooling rate after sintering and getting a hardened part. Due to the porosity of the PM parts, it is generally not possible to quench them in water or oil, fast cooling process is carried out in the sintering equipment, both for batch and continuous furnaces.Even though batch furnaces offer an improved cooling rate control, industrial sintering is typically carried out in belt-furnaces, due to production capability. Belt-furnaces used for sinter hardening are connected with a so called rapid cooling unit (RCU). In this RCU a turbulent gas flow is generated by a gas tight fan. The fan is connected to the bottom of the unit in order to extract the process gas from below the belt. Before the gas reaches the fan, it is cooled down by a heat exchange system. After being accelerated by the fan it is cooled a second time, before reaching the parts. Cooled process gas is used to “quench” the parts entering the RCU. Different cooling

DOI 10.12776/ams.v19i4.181 p-ISSN 1335-1532
e-ISSN 1338-1156

rates can be achieved by adjusting different parameters of the rapid cooling chamber, in this investigation nozzle field tilting and valve opening were kept constant, getting different cooling rates only with fan speed adjusting. The rapid cooling chamber is circulating the sintering atmosphere in a very turbulent way. Thereby cooling rates of 1 °C/s to 5 °C/s in a temperature range of 800˚C to 300˚C can be achieved. Those cooling rates are yet too slow in order to reach a martensitic microstructure within unalloyed steel. It is therefore of great importance to use alloyed steel powders, which are suitable for evolving an almost fully martensitic microstructure under those cooling conditions .Several parameters are influencing this process (powder composition, carbon content, sintering atmosphere, cooling rate, ...) [8, 9], eventually resulting in so-far unexplored new applications for PM components [10].

One powder system showing good sintering hardening behaviour, a sintering atmosphere and a sintering cycle have therefore been selected and kept constant during the whole study whilst experimental efforts have been focused on the analysis of actual cooling rate for different components geometry and density at different RCU settings. Main purpose of this work has therefore been to find a correlation between part geometry (through the definition of a A/M geometry index) and actual cooling rate.

2 Material and experimental methods

A extended set of sinter-hardening cycles have been carried out re-enacting real industrial conditions; to do so a Cremer-Ofenbau belt-furnace equipped with a rapid cooling unit (RCU) has been used. In the RCU, the cooling is achieved by the flow of a turbulent gas, generated by a gas tight fan, the cooling rate depends on the speed of the fan. Sintering has been carried out at 1120°C in a 90:10 nitrogen/hydrogen atmosphere. The material used for the experiments was Hoganas Distaloy DH with an addition of 0,6% w. of graphite and of 0,8 % w. of Acra-wax as lubricant. The Distaloy DH is produced by diffusion bonding 2% copper to Astaloy Mo (itself pre-alloyed with 1,5% molybdenum). This double alloying technique ensures a good compressibility and a small scattering of dimensions [11].

The influence of geometry and dimensions on the actual cooling rate and then on the final microstructure of a selected set of components at different setting of fan speed was analysed introducing a parameter called A/M (Area/ Mass). During hardening, a given quantity of heat has to be dissipated in order to actually cool down the part, this heat has to leave the part through the surface towards the cooling atmosphere. The simple concept of the volume or mass involved is therefore under-defining the real features of a component, whilst other parameters, such as geometry indexes, could provide a better identification and help in the optimization of the production steps [12]. The use of the geometrical modulus, usually describing a given geometry in terms of specific surface (surface area/mass) is helping in classifying items according to the tendency towards surface mechanisms (heat transfer, surface reactions..) for a given volume. This approach is not specific of diffusive processes, such as sintering. The first attempt to index parts geometries was carried out by Chvorinov [13] in order to understand the solidifying process of a cast part as determined by the molten volume and its cooling surface mutual relation. The application of a similar approach to sintered components is hindered by the complexity of the problem and by the number of variables involved, such as compaction pressure, density and many process ones [14-17].

Basically the cooling takes place through the surface area of a part. Therefore, parts with a big surface area should cool down faster than parts with a small surface area by considering same material, density and kind of surface. On the other hand, the higher the mass of a part the more

DOI 10.12776/ams.v19i4.181 p-ISSN 1335-1532
e-ISSN 1338-1156

heat is stored inside and has to be dissipated. Absolute A/M-indexes are simply calculated by dividing the exposed surface area by the mass, whilst relative A/M-indexes are relating to the TS-bar (set as "1") which is used as reference. Selected components consisted in tensile-strength (TS) and impact energy test specimen (IE and LIE) and disc shaped components (C40H and C40L). Moreover, a lowered cylindrical component, C40LL has been introduced to compare its behaviour after sintering with IE bars in order to find if there is any influence of the actual shape on the A/M index. Components were compressed at standard commercial densities of 6,9, 7,0 and 7,1 g/cm^3 achieved compacting at 500, 600 and 800 MPa, covering the range of possible densities achieved from customers [18] and give a rather complete point of view. All dimension and parameters are summarized in the following **Table 1**.

Table 1 Components with different absolute (ρ = 7g/cm^3) and rel. A/M Indexes

Component	**Abbrev.**	**Standard / Dimension [mm]**	**Rel. A/M**
Tensile-strength test bar	TS	ISO 2740 (shaft 6 x 6)	1,0
Impact energy test bar	IE	ISO 5754 (10 x 10 x 55)	0,6
Lowered Impact energy test bar	LIE	Height: 6 mm	0,9
Cylinder	C40H	Ø 40 mm height: 20 mm	0,3
Cylinder	C40L	Ø 40 mm height: 7 mm	0,5
Cylinder	C40LL	Ø 40 mm height: 5 mm	0,6
Material	Distaloy DH + 0,6% C + 0,8% A-Wax		
Compaction pressure	500 MPa	600 MPa	800 MPa

Several sintering cycles have been carried out with same sintering condition, cooling rate have been changed setting four different fan speed (10%, 20%, 50%, 80% of the maximum fan speed achievable). Loading of trays and distance between part were kept constant (210 g and 8 mm).
Different experiments were carried out in order to deeply understand the cooling process, such as determination of a correlation between the imposed fan speed and the actual cooling rate of components, influence of part geometry and density.
Actual cooling rates can be determined in different ways, either using thermocouple (TC) measurements or via metallographic investigations with a comparison of the phase amounts of the quenched components to dilatometer experiments of the same material [19].
To do so a metallographic sample has been obtained from the centre of selected components and the amount of each phase quantified by means of point analysis, (200x magnification on a 5 x 5 grid) the resulting amount of martensite was then compared to the dilatometer curve taken from the Höganäs AB database for Distaloy-DH with the same percentage of graphite to find the corresponding cooling rates [11, 20].
An additional TC test was carried on in order to verify how much the actual cooling profile can be affected from exothermical bainitic reaction taking place as shown from dilatometric experiment.
Sintering with same parameters and 25% fan speed has been run while TC measuring was executed in the atmosphere and in TS samples both of DH and of pure iron (ASC 100.29).

DOI 10.12776/ams.v19i4.181 p-ISSN 1335-1532
e-ISSN 1338-1156

The trial was repeated with and without perforated trays; in the trial without trays, samples were placed directly on the belt keeping constant distance between parts.
The experiment without trays was carried on in order to see any influence of the boat on the heat transfer or in the flow of cooling medium.
In order to further deepen the understanding of the phenomena underneath the sinter-hardening processes, other analysis have been carried out on sintered components, such as oxygen and carbon content, hardness and micro-hardness measurements [21].
Chemical analysis in order to determine the percentage of carbon and oxygen was carried out in the as-sintered state. One gram of each specimen and powder mix has been examined for all cooling rates using Leco CS 444 and Leco TC 600 analysers according to ISO 15 351and ISO 15 350 respectively.
Samples hardness was measured using Vickers HV10 scale, according to ISO 6507 and ISO 4498, while the load time was 15s and the load speed was 150 μm/s. For each specimen six indents on the top surface (the one exposed to the quenching gas) and another six on the bottom surface were examined. Microhardness measurement was done in order to be able to judge the possibility of decarburization during sintering. The microhardness was measured in one phase only. It was necessary to judge the difference between martensite and bainite, but yet being able to make a clear indentation. Therefore, the etching was carried out appropriately. Six indentations on the top, bottom and in the centre were examined. All measurements were done according to ISO 4516 and ISO 4498 with a Matsuzawa MMT-7. Vickers hardness was examined with a load of 50g. The load was chosen in order to place an indent in one phase only, while the higher load was preferred.

3 Results and discussion

3.1 Chemical Analysis

The mean amount of final carbon and oxygen content in the as-sintered state resulted to be quite stable among samples compacted at different densities, with a constant loss in terms of carbon content resulting in an average value of 0,57 %w. This decarburization didn´t result in any compositional profile but homogeneous at all distances from the surface, as confirmed from microhardness analysis.

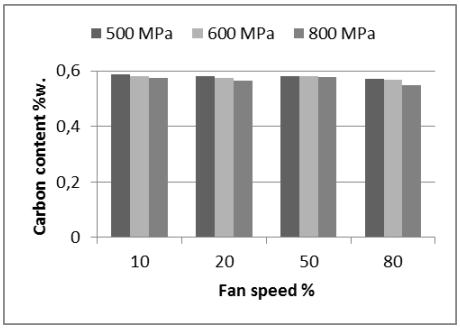

Fig.1 Carbon content at different fan speed.

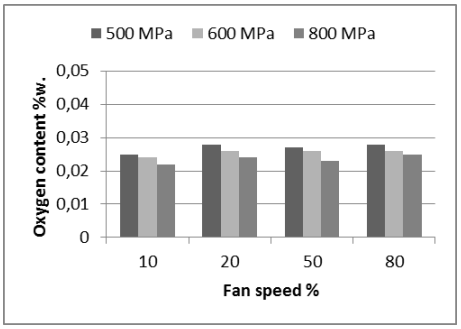

Fig.2 Oxygen content at different fan speed.

The difference in oxygen and carbon content after sintering at different fan speed can be related to the oxygen content in the atmosphere. During all trials risk of oxidation has therefore been

DOI 10.12776/ams.v19i4.181 p-ISSN 1335-1532
e-ISSN 1338-1156

investigated controlling the atmosphere composition in the rapid cooling unit. Results deriving from an oxygen probe connected at the top of RCU are summarized in the following **Table 2**.

Table 2 Measured Dew Point

Fan Speed	Signal [mV]	Dew point
10%	1361	-61°C
20%	1325	-55 °C
50%	1326	-55°C
80%	1331	-56°C

Lower dew point, and thus better reducing conditions, has been achieved sintering at 10% of fan speed. The use of low fan speed allows a better mixing of the atmosphere avoiding leakages from entrance and exit of the furnace. Furthermore, worse condition at higher fan speed can be explained considering that such an high fan speed leads to sucking of air from the outside.

3.2 Metallographic investigation

Metallographic analysis revealed a microstructure mainly constituted of upper-bainite and martensite. In order to evaluate phase amount, metallographic samples were observed via point-analysis and main resulted related to the detected amount of martensite are reported in the following **Fig. 3**.

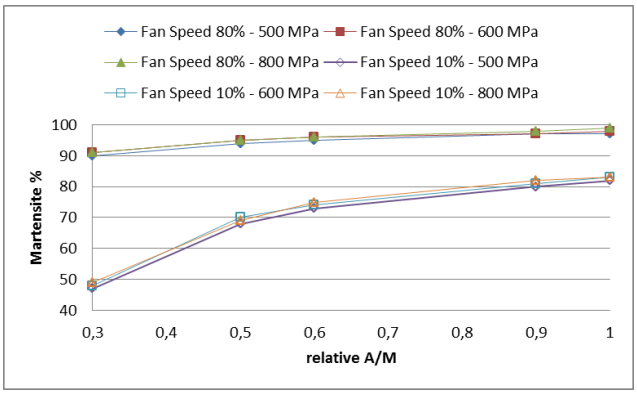

Fig.3 Martensite amount for different shapes and compactions pressures

Phase analysis doesn't reveal any strong correlation between density and final microstructure neither on parts with high nor low A/M index. On the other hand, a strong correlation has been observed when considering the obtained microstructure as a function of the geometrical index.

Given the higher specific surface, parts with high A/M index, revealed an higher tendency towards the development of martensitic structures. Tensile test bars (TS) and lowered Impact energy bars (LIE), respectively 1.0 and 0.9 relative A/M index, reached up to 80% of martensitic microstructure even fot the lowest fan speed (10%) as reported in **Fig. 3**.

Parts with high A/M index are cooled down faster than parts with a low index, that forming an higher amount of martensite. The resulting phase amounts don´t change significantly between the centre and the edge of the considered sample.

Considering C40H samples cooled with a fan speed of 20%, comparing 500 MPa and 800 MPa pressure , it is possible to notice same microstructure (approximately 60% of martensite), as shown in following **Fig. 4** and **Fig. 5**.

DOI 10.12776/ams.v19i4.181 p-ISSN 1335-1532
e-ISSN 1338-1156

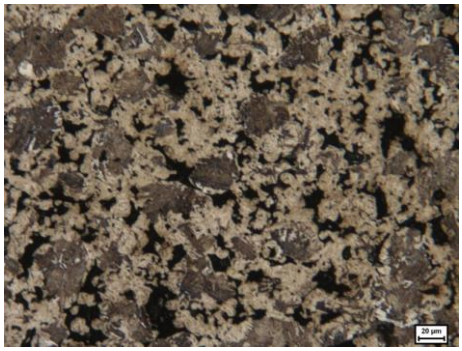

Fig.4 C40H, 500 MPa, 20% fan speed

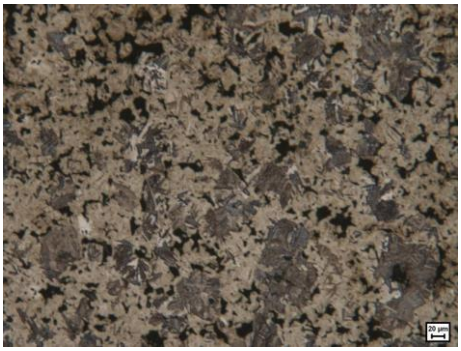

Fig.5 C40H, 800 MPa, 20% fan speed

Even evaluating parts with a lower A/M index the same behaviour is detected. TS bars, cooled down with 20% fan speed compacted with 500 MPa and 800 MPa show comparable amount of martensite, approximately 85%, as shown in following **Fig. 6** and **Fig. 7**.

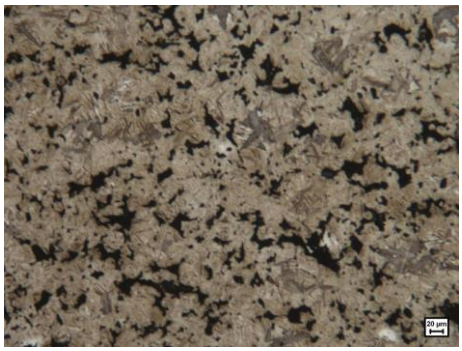

Fig.6 TS bar, 500 MPa, 20% fan speed

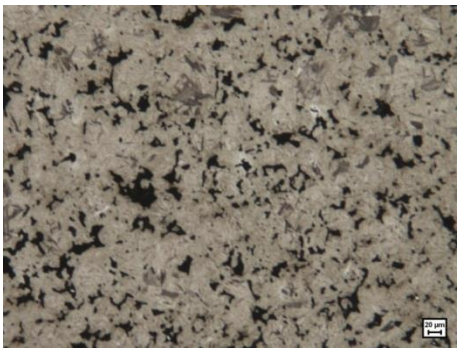

Fig.7 TS bar, 800 MPa, 20% fan speed

No influence of the density on the structure was noticed using increasing fan speed: cooling down at 80% fan speed, C40H samples compacted at 500 MPa show same structure than C40H compacted at 800 MPa (91% martensite), as shown in following **Fig. 8** and **Fig. 9**.

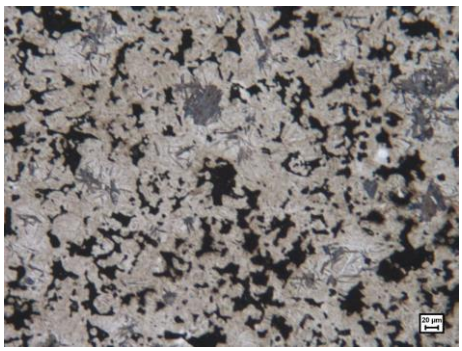

Fig.8 C40H, 500 MPa, 80% fan speed

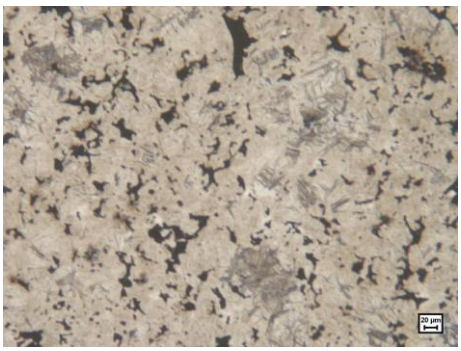

Fig.9 C40H, 800 MPa, 80% fan speed

In addition, comparison of different geometries with the same A/M index confirms the reliability of the index: parts with same value of the index but different shapes show same microstructure.

DOI 10.12776/ams.v19i4.181 p-ISSN 1335-1532
e-ISSN 1338-1156

In **Fig. 10** and **Fig. 11**, showing IE bar and C40LL cylinder compacted at the same density and with same A/M index (0,6) , it is possible to notice that the microstructure is approximately the same (95% martensite)

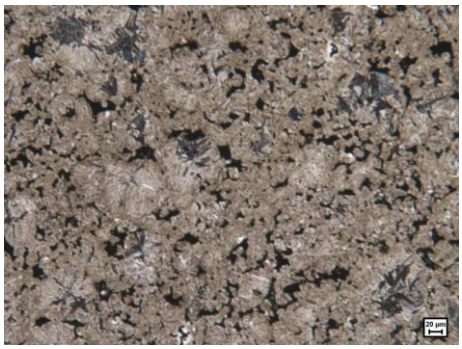

Fig.10 IE bar ,600 MPa, 80% fan speed

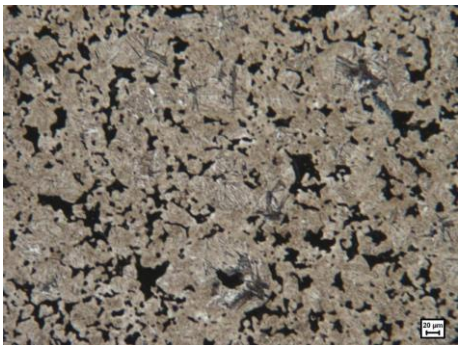

Fig.11 C40LL, 600 MPa, 80% fan speed

3.3 Apparent Hardness

The difference in hardness measured on the top and on the bottom of specimens never exceeded 10% therefore only mean values were considered and summarized in the following **Fig. 12**.
Samples compacted with an higher pressure presented an higher apparent density and a minor difference in hardness achieved at different fan speed

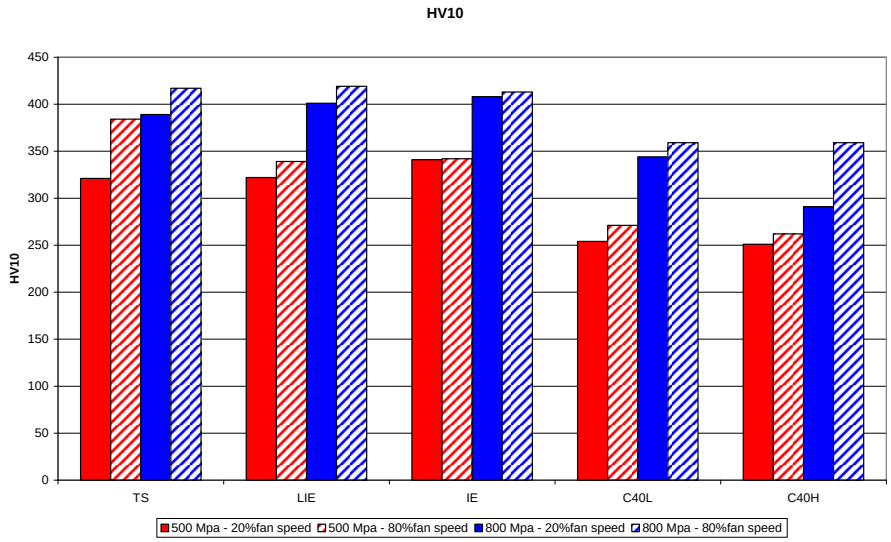

Fig.12 Hardness Vickers 10, measured on TS bars achieved at different fan speed on components with different density

3.4 Micro hardness

Microhardness analysis has been carried out on TS and LIE bars, showing consistent amounts of martensite even at low fan speed. In order to have comparable values only fully martensitic areas have been tested.
The results are presented in **Table 3**.

DOI 10.12776/ams.v19i4.181 p-ISSN 1335-1532
e-ISSN 1338-1156

Table 3 Microhardness values

Upper			Lower		
TS	**500 [Mpa]**	**800 [Mpa]**	**TS**	**500 [Mpa]**	**800 [Mpa]**
20	624	607	**20**	701	744
50	667	606	**50**	658	696
80	694	693	**80**	696	686
LIE	**500 [Mpa]**	**800 [Mpa]**	**LIE**	**500 [Mpa]**	**800 [Mpa]**
20	685	646	**20**	614	624
50	687	647	**50**	649	630
80	681	635	**80**	651	667

3.5 Iron test

In order to verify the influence of the exothermical bainitic reaction shown by dilatometric analysis, on the actual cooling rate measured via TC, additional sintering trials have been set up. Cycles with 25% fan speed have been run while TC measuring were executed both in the atmosphere and in TS samples. Test was carried out with both Distaloy -DH and ASC 100.29 (pure iron) samples , with and without the use of perforated trays. In the trial without trays samples were placed directly on the belt keeping constant distance between parts.

The experiment without trays was carried on in order to see any influence of the boat on the heat transfer or in the flow of cooling medium.

Cooling profiles were recorded for both trials, three thermocouples were used: two of them were placed in TS bars (one of ASC and one of DH) and one was placed in the atmosphere.

The cooling profile inside the RCU is presented in the following **Fig. 13**.

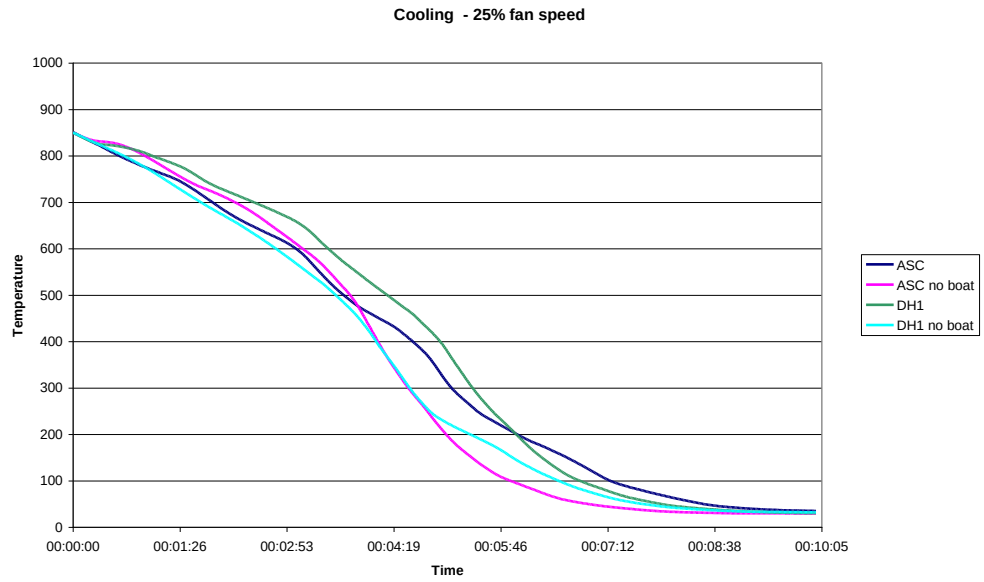

Fig.13 Cooling profile inside the RCU

Mean cooling rate between 800 and 300°C was measured, **Table 4**.

DOI 10.12776/ams.v19i4.181 p-ISSN 1335-1532
e-ISSN 1338-1156

Table 4 Mean cooling rate measured in different conditions

	cooling rate [°C/sec]
ASC	1,85
ASC no boat	2,35
DH	1,93
DH no boat	2,16

3.6 Cooling rate evaluation

During experimental activity, several parameters and their mutual relations have been considered.

As mentioned before, the main goal of this work was to further deepen the knowledge on the sinter-hardening process in real-like conditions. The actual system is therefore playing a key-role in the definition of a possible correlation between set parameters (density, part geometry, fan speed, …) and the final output of the process in terms of final micro-structure and consequently mechanical properties.

An additional effort had to be done in order to extend the derived information on an enlarged scale and create a tool able to correlate actual cooling information to producers datasheet [11, 20-23].

All the aforementioned analysis have then been summarized in the following graph (**Fig. 14**), merging available dilatometer data with the measured values.

For each specific system (in terms of powder and sintering conditions), knowing geometry features of the parts and the desired amount of martensite the proper cooling conditions can be easily identified.

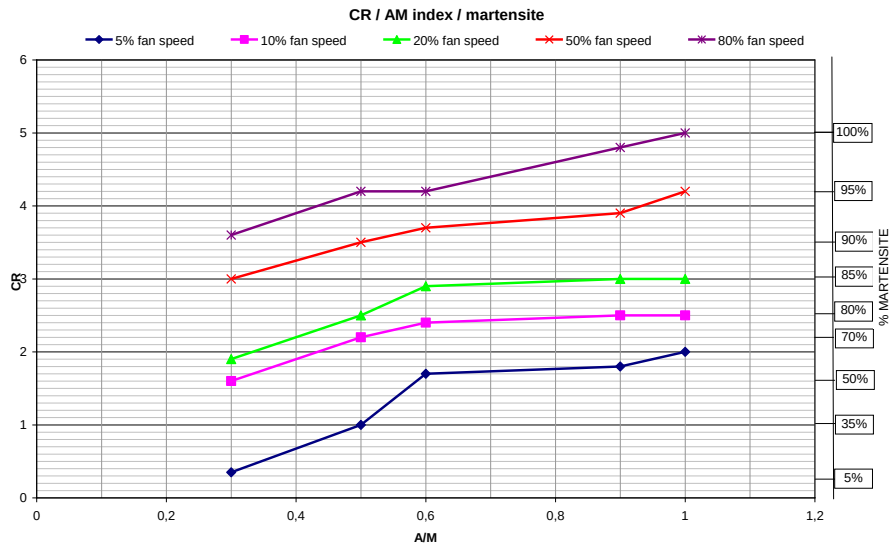

Fig.14 Cooling rate/microstructure graph for DH for different geometries.

4 Conclusions

When talking about cooling rate, the modality of determination is very important, as shown before actual cooling rate can be measured using thermocouples directly in the sample.

DOI 10.12776/ams.v19i4.181 p-ISSN 1335-1532
e-ISSN 1338-1156

Comparing the microstructure obtained and its actual cooling rate with atlas achieved by dilatometric investigations, rather big differences can be found.
This can be explained since the dilatometer is a closed-system where the amount of heat is the imposed varying parameter, furthermore this kind of investigation is usually run on small samples where any influence of the mass is negligible.
From the analysis of the cooling profile inside the rapid cooling unit, short disturbance are found, this can have huge effects on the final microstructure when appearing at sensitive temperature ranges.
It is possible to state that these disturbance aren't related to bainitic transformation in the material but are probably connected with the flow of the cooling medium in the chamber since they appear also when using pure iron.
If a certain amount of martensite is desired, the comparison to the constant dilatometer curve will still be the method of choice.
This investigation tries to give a preliminary overview of the cooling characteristic of the investigated belt furnace and to draw a graph tool correlating cooling rate, determined by dilatometer, with the microstructure that is possible to achieve for different parts.

References

[1] E. Dudrova, M. Kabatova, R. Bidulsky: Metalurgija, Vol. 42, 2003, No. 1, p. 3-20
[2] E. Dudrova, M. Kabatova, S.C. Mitchell, R. Bidulsky, A.S. Wronski: Powder Metallurgy, Vol. 53, 2010, No. 3, p. 244-250
[3] R. Bidulsky, E. Dudrova, M. Kabatova: Deformation and Fracture Behaviour of Sintered Manganese Steels. In: DFPM 2002, Ľ. Parilák, H. Danninger (Eds.), IMR SAS, Košice, 2002, Vol. 2, p. 31-34
[4] J. Bidulska, R. Bidulsky, M. Actis Grande: Acta Metallurgica Slovaca, Vol. 16, 2010, No. 3, p. 146-150
[5] I. Nyberg, M. Schmidt, P. Thorne, J. Gabler, T.J. Jesberger, S. Feldbauer: Effect of Sintering Time and Cooling Rate on Sinterhardenable Materials, In: PM2Tec2003, Advances in Powder Metallurgy and Particulate Materials – 2003, MPIF, Princeton, 2003
[6] W. B. James: What is Sinter-Hardening?, In: PM2Tec'98, Advances in Powder Metallurgy and Particulate Materials – 1998, MPIF, Princeton, 1998
[7] E. Dudrova, M. Kabatova, R. Bidulsky, A.S. Wronski: Powder Metallurgy, Vol. 47, 2004, No. 2, p. 181-190
[8] O. Bergman, B. Lindqvist, S. Bengtsson: Materials Science Forum, Vol. 534-536, 2007, p. 545-548
[9] M. Schmidt, P. Thorne, U: Engström, J. Gabler, T.J. Jesberger, S.Feldbauer: Effect of Sintering Time and Cooling Rate on Sinter Hardenable Materials, In: PM2Tec2004, MPIF, Princeton, 2004
[10] M. Maccarini, R. Bidulsky, M. Actis Grande: Acta Metallurgica Slovaca, Vol. 18, 2012, No. 2-3, p. 69-75
[11] Höganäs handbook for sintered components: 1. Material and powder properties, Höganäs AB, 2004
[12] U. Engström, D. Milligan, A. Bergmark, S. Bengtsson, B. Maroli: Evaluating the Effect of Mass on the Sinter-Hardening Response of Various PM Steels In: PM2Tec2006, MPIF, Princeton, 2006

DOI 10.12776/ams.v19i4.181 p-ISSN 1335-1532
e-ISSN 1338-1156

[13] F.Havlicek, T. Elbel, Archives of Foundry Engineering, Vol.11, 2011, No. 4, p. 170-176
[14] G. Bocchini, M. Pinasco, B. Rivolta B, G.Silva: International Journals of Materials and Product Technology, Vol. 28, 2007, No. 3-4 , p. 312-337
[15] J.C.Y. Koh, A. Fortini: International Journal of Heat and Mass Transfer, Vol. 16, 1973, No.11, p. 2013-2022
[16] Ö.E. Ataer, C. Aygün, İ. Uslan: Powder Technology, Vol. 137, 2003, No. 3, p. 159-166
[17] S. Saritas, R.D. Doherty, A. Lawley: International Journal of Powder Metallurgy, Vol. 38, 2002, No. 1, p. 31-40
[18] Höganäs handbook for sintered components: 2. Production of sintered components, Höganäs AB, 2004
[19] M.A Pershing, H. Nandi, A methodology for evaluating sinter-hardening capability, In: PM2Tec'01, MPIF, Princeton, NJ, 2001
[20] Höganäs handbook for sintered components. 6. Metallography, Höganäs AB, 1999.
[21] J. Arvidsson, A. Tryggmo: Metal Powder Report, Vol. 54, 1999, No. 2, p. 41
[22] R. Bidulský, M. Actis Grande, J. Bidulská, T. Kvačkaj: Materiali in Tehnologije, Vol. 43, 2009, No. 6, p. 303-307
[23] E. Dudrová, M. Kabátová, R. Bureš, R. Bidulský, A.S. Wronski: Kovové Materiály, Vol. 43, 2005, No. 6, p. 404-421

DOI 10.12776/ams.v19i4.181 p-ISSN 1335-1532
e-ISSN 1338-1156